Listening to Cell Membrane Potential: a new diagnostic and interventional ultrasound imaging approach

Emad M. Boctor, Ph.D.
Assistant Professor of Radiology,
Computer Science, and Electrical Engineering Departments
Director of the Medical Ultrasound Imaging and Intervention Collaboration (MUSiiC) Research Laboratory

Collaborators: Arthur Burnett, Peter Gehlbach, Maged Harraz, Jin Kang, Dean Wong, Arman Rahmim, Les Loew
MUSiiC Lab Members: Jeeun Kang, Kai Zhang

July 16th 2019

JOHNS HOPKINS UNIVERSITY | JOHNS HOPKINS SCHOOL of MEDICINE | MUSiiC Research Laboratory

Neuro-transmitter (NT) and electrophysiological change

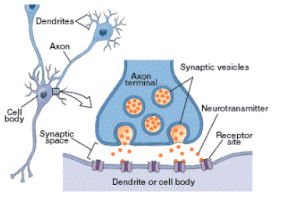

1. Synthesis of the neurotransmitter. This can take place in the cell body, in the axon, or in the axon terminal.
2. Storage of the neurotransmitter in storage granules or vesicles in the axon terminal.
3. Calcium enters the axon terminal during an action potential, causing release of the neurotransmitter into the synaptic cleft.
4. After its release, the transmitter binds to and activates a receptor in the postsynaptic membrane.
5. Deactivation of the neurotransmitter. The neurotransmitter is either destroyed enzymatically, or taken back into the terminal from which it came, where it can be reused, or degraded and removed.

- Action potential; clue of NT event
  - msec time scale
  - -70~40 mV voltage change

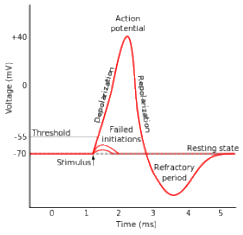

2

Functional neuro-sensing

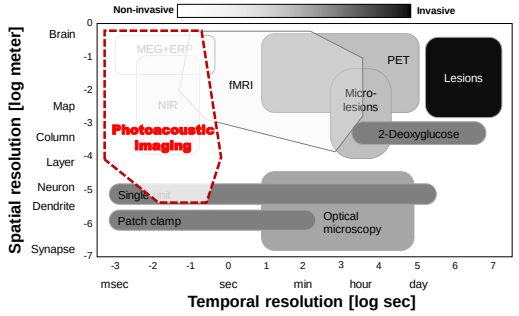

Reproduced from Cohen M. S. and Bookheimer S. Y., *Trends Neurosci* **17**(7), 268-77 (1994).
† Wang L. V. and Song H., *Science* **335**(3075), 1458-1462 (2012).

3

Functional neuro-imaging

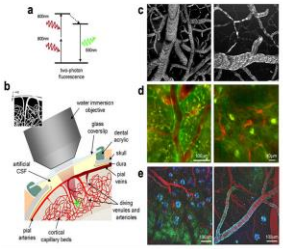

Optical imaging (e.g., two photon microscopy): shallow imaging depth due to diffraction limit (< 1mm), necessitates craniotomy to have sufficient sensitivity

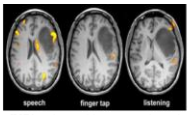

fMRI: only provide contrast based on blood oxygen-level dependent (BOLD) signals

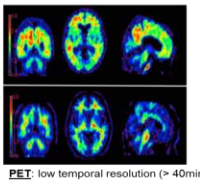

PET: low temporal resolution (> 40min)

Photoacoustic effect

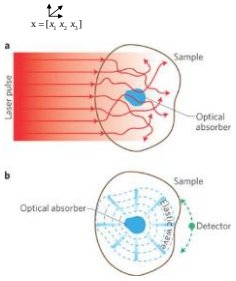

- **Equation of state**

  → Temperature T, density ρ, pressure p

  (In fluid with homogeneous thermodynamic property)

$$\frac{\partial p}{\partial t} = \frac{1}{\rho k_T}\frac{\partial \rho}{\partial t} + \frac{\beta}{k_T}\frac{\partial T}{\partial t}$$

  ρ: mass density [kg/m^3]

  k_T : isothermal compressibility [$\Delta V/V$]

  β: volume thermal expansivity of the fluid [$\Delta V/(V \cdot K)$]

- **Heat equation**

$$\rho C_v \frac{\partial T}{\partial t} = -\chi \nabla^2 T + H(x) f(t)$$

  χ : Thermal conductivity [W/(m · K)]

  C_v : Heat capacity at constant volume [$J/(kg \cdot K)$]

  $H(x)$: Absorbed energy density [J/m^3]

  $f(t)$: temporal pulse shape function with unit integral [/s]

5

Photoacoustic effect

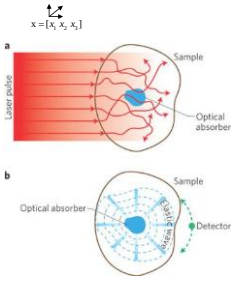

$$\frac{\partial p}{\partial t} = \frac{1}{\rho k_T}\frac{\partial \rho}{\partial t} + \frac{\beta}{k_T}\frac{\partial T}{\partial t}$$ *Equation of state*

↓ **stress confinement (~ns)** $\frac{\partial \rho}{\partial t} << \frac{\partial T}{\partial t}$

Isochoric condition (fixed volume)

$$\frac{\partial p}{\partial t} = \frac{\beta}{k_T}\frac{\partial T}{\partial t}$$

Heat equation

$$\rho C_v \frac{\partial T}{\partial t} = -\chi \nabla^2 T + H(x) f(t) \Rightarrow \frac{\partial T}{\partial t} = \frac{1}{\rho C_v} H(x) f(t)$$

↓ **thermal confinement (~μs)**

→ **Heat delivery faster than conductive heat diffusion**

$$\frac{\partial p}{\partial t} = \frac{\beta}{\rho C_v k_T} H(x) f(t)$$

↓ Integral over **short pulse duration**

$$p_0 = \frac{\beta}{\rho C_v k_T} H(x) = \Gamma H(x) = \Gamma \mu_a \Phi(x)$$

6

Towards sensing electrophysiological activity in deep brain

- **Objective:** real-time, transcranial photoacoustic (PA) sensing of electrophysiological brain activity at deep rat brain *in vivo*
- Voltage-sensing mechanism using near-infrared cyanine dye [†]

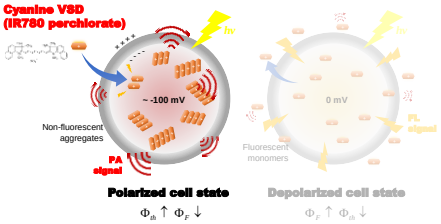

- Cyanine dye with positive polarity is attracted into cell membrane
- The aggregation of VSD leads to fluorescence (FL) quenching, which **increases PA generation efficiency**

[†] Zhang, H. K. *et al. J. Biomed. Opt.* **22,** 045006 (2017).

Towards sensing electrophysiological activity in deep brain

- **Objective:** real-time, transcranial photoacoustic (PA) sensing of electrophysiological brain activity at deep rat brain *in vivo*
- Voltage-sensing mechanism using near-infrared cyanine dye [†]

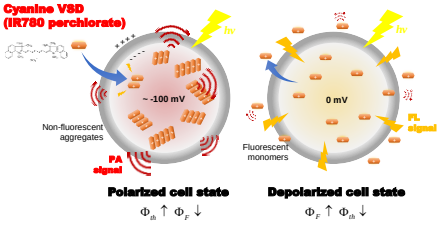

- Dispersion of VSD gives **high FL efficiency**

[†] Zhang, H. K. *et al. J. Biomed. Opt.* **22,** 045006 (2017).

VSD characterization using artificial membrane potential model

- Artificial membrane diffusion potential model [†][†]

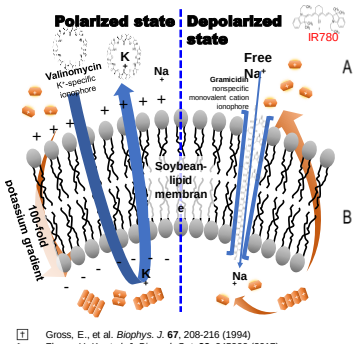

***In vitro* VSD characterization (6μM).** (A) Absorbance and fluorescence emission spectrum of near-infrared VSD. (B) Photoacoustic spectrum and intensity change at the 790 nm of peak absorbance.

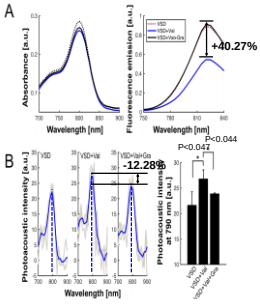

[†] Gross, E., et al. *Biophys. J.* **67**, 208-216 (1994)
[†] Zhang, H. K. *et al. J. Biomed. Opt.* **22,** 045006 (2017).

In vivo experimental setup

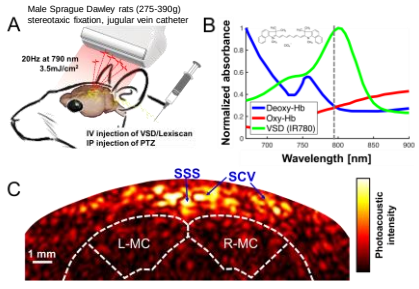

10

In vivo experimental protocol

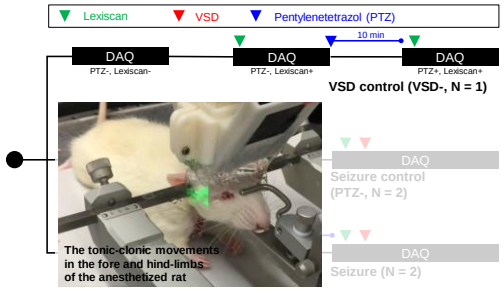

11

In vivo photoacoustic VSD imaging

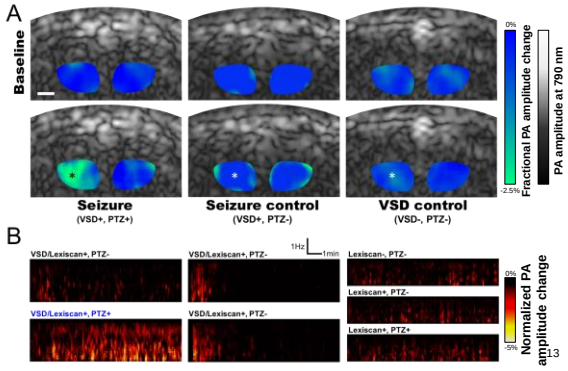

13

In vivo photoacoustic VSD imaging

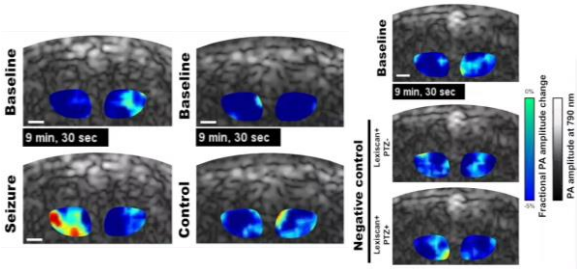

14

Visual cortex stimulation and monitoring

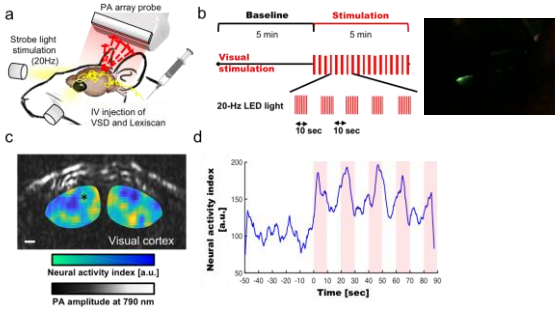

15

Visual cortex stimulation and monitoring

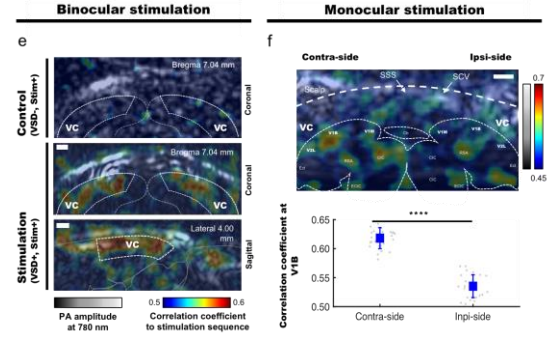

16

From Brain to Prostate

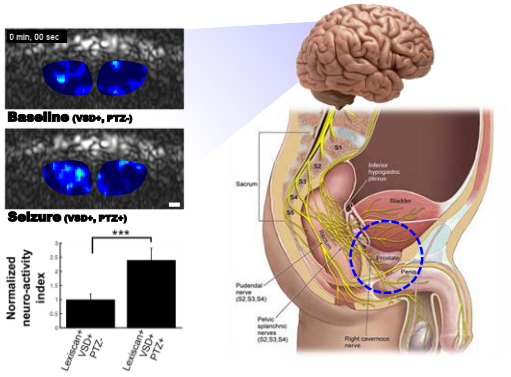

17

Need for nerve guidance during peeling out procedure of fascia

18

Proposed nerve-guided robot-assisted laparoscopic prostatectomy

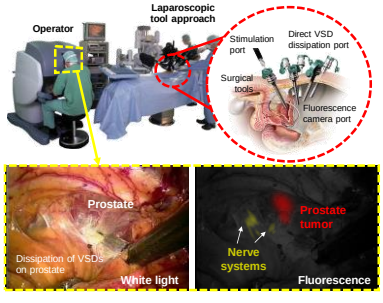

Step 1: Robotic tool approach through the ports on the abdominal incisions,

Step 2: Direct VSD staining of a prostate tissue through the abdominal incision port,

Step 3: Flushing out of the VSD on the prostate surface which is not bound at tissue membrane,

Step 4: Stimulation on nerves in the surgical region-of-interest, and

Step 5: Nerve-sparing prostatectomy with the augmented nerve map

19

Available time for VSD staining

- Dissection of colon adhesions ~0:31
- Posterior approach with dissection of the seminal vesicles ~2:47
- Dissection of the anterior abdominal wall~10:50
- Opening of the endopelvic fascia and dissection of the periprostatic fat
- **Suture of the dorsal venous complex** — 8-10 min
- **Preservation of neurovascular bundles during left sided dissection**
- Dissection of the left posterior pedicle ~33:20
- Apical and urethral dissection ~49:01
- Evaluation of nerve sparing with the ProPep electrodes ~54:14
- Vesicourethral anastomosis ~55:12
- Surgery ended ~1:07

Time point completing exposure of prostate capsuled with periprostatic fascia

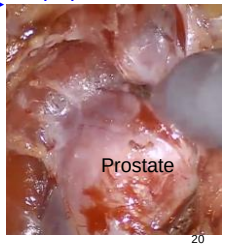

20

In vivo experimental protocol

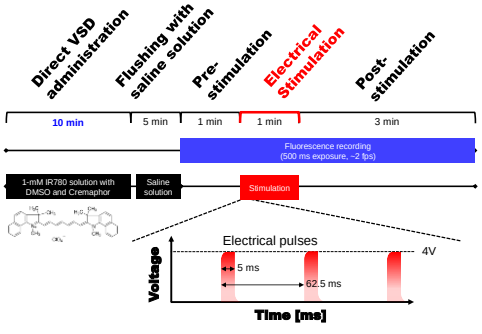

21

In vivo experimental setup

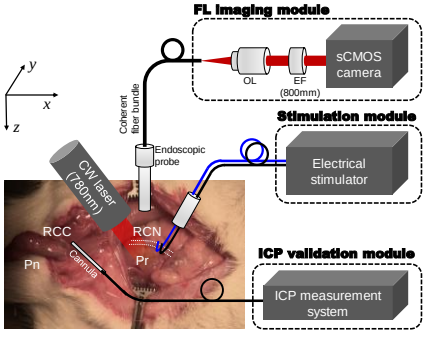

Pr: prostate; Pn: penis; RCN: right cavernous nerve; RCC: right corpus cavernosum
ICP: intracavernos pressure

22

Validation of erectile stimulation

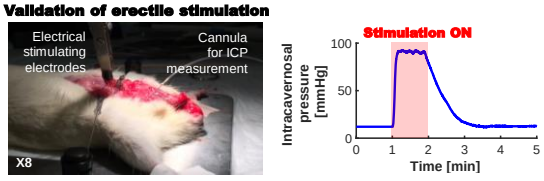

23

Real-time prostate nerve mapping *in vivo*

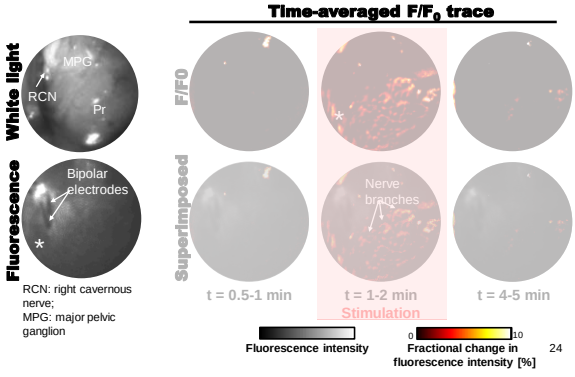

RCN: right cavernous nerve;
MPG: major pelvic ganglion

24

Real-time prostate nerve mapping *in vivo* (2nd attempt)

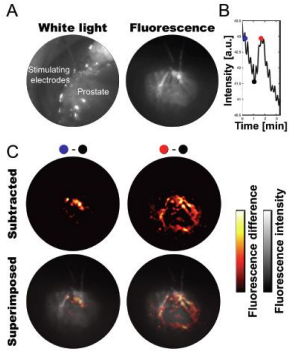

Preliminary *in vivo* results on nerve localization on rat prostate:

(A) White light and FL images;
(B) Evolution of FL intensity during stimulation. The gradual decrease is due to photo-bleaching;
(C) Subtracted images between indicators, and its fusion on FL images.

Histological validation of direct VSD administration

- Confirmed direct staining procedures can deliver VSD > 2-mm deep in prostate

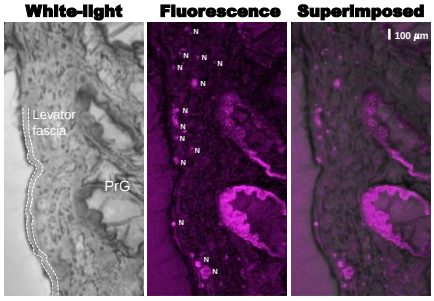

26

Discussion

- We presented the preliminary results of real-time nerve guidance using dual-modal VSD and intra-operative FL imaging

- Our further works will be focused on
  - Developing pulsed laser-based dual-modal intra-operative guidance

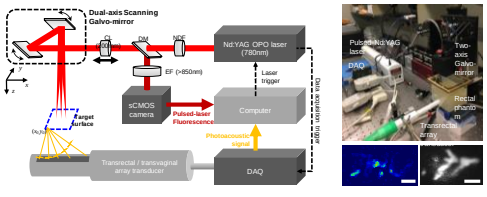

27

Discussion

- We presented the preliminary results of real-time nerve guidance using dual-modal VSD and intra-operative FL imaging

- Our further works will be focused on
  - Developing pulsed laser-based dual-modal intra-operative guidance
  - Integrating non-invasive ultrasound neuromodulation

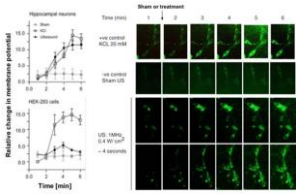

28

Discussion

- We presented preliminary results of real-time nerve guidance using dual-modal VSD and intra-operative FL imaging

- Our further works will be focused on
  - Developing pulsed laser-based dual-modal intra-operative guidance
  - Integrating non-invasive ultrasound neuromodulation
  - Constructing control group with CN block

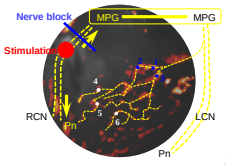

29

Discussion

- We presented the preliminary results of real-time nerve guidance using dual-modal VSD and intra-operative FL imaging

- Our further works will be focused on
  - Developing pulsed laser-based dual-modal intra-operative guidance
  - Integrating non-invasive ultrasound neural stimulation
  - Constructing control group with CN block
  - Evaluating nerve trauma with VSD sensing

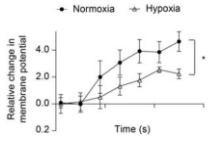

30

Thank you

31

Quantitative comparison

- Normalized neuro-activity index (projected during 2-10 min)

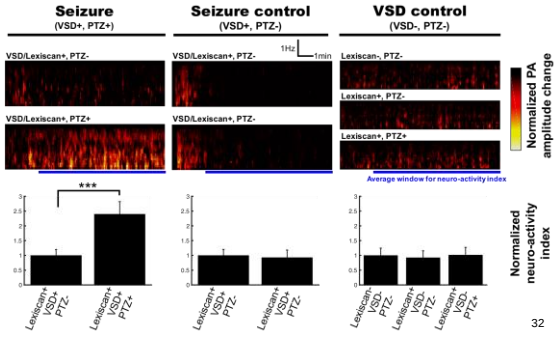

Photoacoustic effect

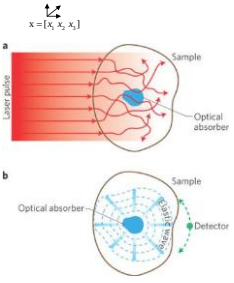

- **Equation of state**

  → Temperature T, density ρ, pressure p

  (In fluid with homogeneous thermodynamic property)

$$\frac{\partial p}{\partial t} = \frac{1}{\rho k_T}\frac{\partial \rho}{\partial t} + \frac{\beta}{k_T}\frac{\partial T}{\partial t}$$

  ρ: mass density [kg/m^3]

  k_T : isothermal compressibility [$\Delta V/V$]

  β: volume thermal expansivity of the fluid [$\Delta V/(V \cdot K)$]

- **Heat equation**

$$\rho C_v \frac{\partial T}{\partial t} = -\chi \nabla^2 T + H(x) f(t)$$

  χ : Thermal conductivity [W/(m · K)]

  C_v : Heat capacity at constant volume [$J/(kg \cdot K)$]

  $H(x)$: Absorbed energy density [J/m^3]

  $f(t)$: temporal pulse shape function with unit integral [/s]

Photoacoustic effect

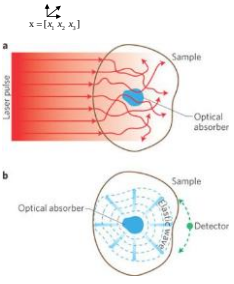

$$\frac{\partial p}{\partial t} = \frac{1}{\rho k_T}\frac{\partial \rho}{\partial t} + \frac{\beta}{k_T}\frac{\partial T}{\partial t}$$ *Equation of state*

↓ **stress confinement (~ns)** $\frac{\partial \rho}{\partial t} << \frac{\partial T}{\partial t}$

Isochoric condition (fixed volume)

$$\frac{\partial p}{\partial t} = \frac{\beta}{k_T}\frac{\partial T}{\partial t}$$ *Heat equation*

$$\rho C_v \frac{\partial T}{\partial t} = -\chi \nabla^2 T + H(x) f(t) \Rightarrow \frac{\partial T}{\partial t} = \frac{1}{\rho C_v} H(x) f(t)$$

↓ **thermal confinement (~μs)**

→ **Heat delivery faster than conductive heat diffusion**

$$\frac{\partial p}{\partial t} = \frac{\beta}{\rho C_v k_T} H(x) f(t)$$

↓ Integral over **short pulse duration**

$$p_0 = \frac{\beta}{\rho C_v k_T} H(x) = \Gamma H(x) = \Gamma \mu_a \Phi(x)$$

Clinical applications

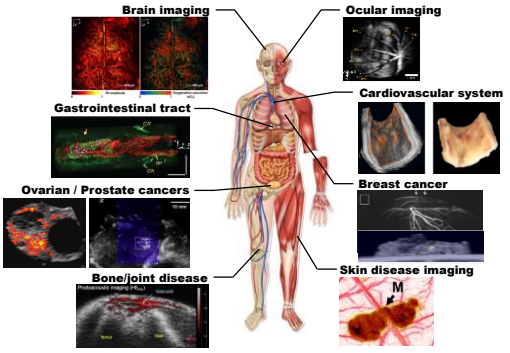

Reproduced from Zackrisson, S., et al., *Cancer Research*, **74**(4), 979–1004 (2014)

EEG confirmation of *In vivo* protocol

- EEG confirmation of seizure induction using PTZ administration

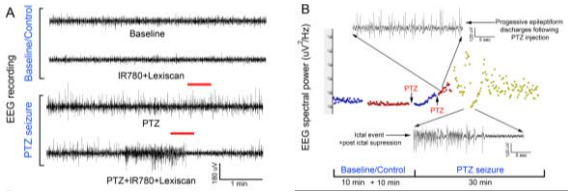

Evolution of EEG signal in the *in vivo* protocol identical to transcranial PA imaging: (A) Representative EEG traces recorded from rat motor cortex before and during induction of status epilepticus using chemoconvulsant PTZ. (B) EEG spectral quantitation of the EEG recording done doe every 10 sec epoch during the EEG showed the expected progressive rise in EEG power associated with evolution of the PTZ induced status epilepticus.

Validation of important assumptions

- Pharmacological treatment for BBB opening
  - Blood-brain barrier (BBB): semipermeable membrane barrier separating the circulating blood from the brain in the central nervous system (CNS)[†]
  - Regadenoson (i.e., Lexiscan™) can modulate adenosine receptor signaling to enhance the permeability of VSD through BBB[†,♀]

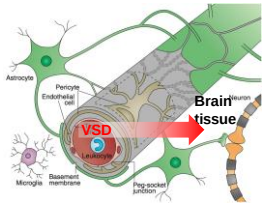

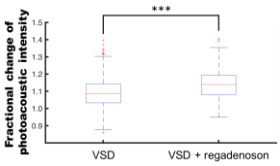

~5% more PA intensity have observed at motor cortex with the systemically injected Lexiscan and VSD. (*N* = 2 for each case)

† Obermeier B., *et al. Nat. Med. Rev.* **19**, 1584-1596 (2013)
† Carman A. J., *et al. J. Neurosci.* **31**(37), 13272-80 (2011).
♀ Bynoe, M. S., et al., *Fluids Barriers CNS* **12**(20) (2015)

Validation of important assumptions

- Robustness on VSD interference on neuro-activity

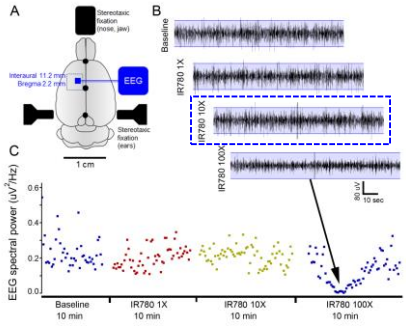

38